Analyzing Mid-Spatial Frequency Error in Monolithic Freeform Telescopes

Design Description Document

Optimax Systems / Todd Blalock

David Henry Lippman	Project Coordinator
Wooyoun Kim	Document Handler
Kevin Kuyk	Customer Liaison
Matthew Page	Scribe
Professor Jannick Rolland	Faculty Advisor

Document Number 00002

Revisions Level	Date
F	05-06-2018

Authentication Block

Revision History:

Revision	Description	Date	Authorization
A	Initial DDD	01-21-2018	DHL
B	Updated DDD	02-03-2018	DHL
C	Updated DDD	02-17-2018	MMP
D	Midterm DDD	02-24-2018	DHL
E	Updated DDD	04-01-2018	DHL
F	Final DDD	05-06-2018	DHL

Table of Contents:

1. Background

Monolithic optical systems offer great promise for a variety of applications by eliminating the possibility of most alignment errors; however, fabricating monolithic systems – especially those containing aspheric or even freeform surfaces – remains a challenge. Mid-spatial frequency (MSF) figure errors are unavoidable artifacts introduced to optical surfaces when performing sub-aperture grinding and polishing, methods typically used for fabricating aspheric and freeform surfaces. Although a variety of techniques can be used to mitigate these features, MSF errors can greatly hinder optical performance in a variety of different ways. Measuring and tolerancing MSF errors introduced during the manufacturing process are key first steps in adequately fabricating these monolithic optical systems. Three monolithic telescope designs being fabricated by Optimax Systems contain multiple freeform surfaces and will be analyzed for sensitivity to MSF error.

The product is a thorough design study and sensitivity analysis of the impact of MSF figure error on the imaging performance on these monolithic freeform telescopes as well as tolerancing what MSF error is allowable for desired optical performance. This is done with a computational model for MSF error that is verified by empirical measurements performed on the freeform telescopes.

2. Methods & Procedure

a) Overview

The project objective is to understand and model how MSF error affects the monolithic telescopes. To do this:

1. First, a model that accurately simulates the effect MSF error has on a system's imaging performance must be created

2. Second, this model must be verified using empirical measurements for confirmation

3. Third, this MSF model can now be applied to the Stage 3 telescope design to perform sensitivity analysis and tolerancing

To create a model that accurately simulates the effect MSF error has on a system, a metric of some sort must be used to correlate between simulated and empirical data. This metric must be able to be calculated using an optical design software like CODE V and must be able to be measured in a lab environment. This metric must also be a measurement that is as independent as possible from other system aberrations, fabrication errors, and anything else that would cause a difference between simulated and measured metrics.

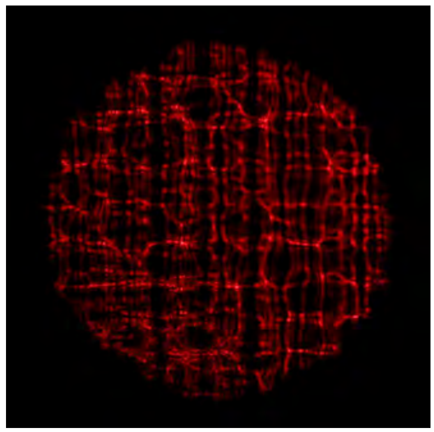

Figure 1: Sample out-of-focus spot containing mid-spatial frequency signatures.

The metric we used to validate our model against empirical measurements is a through-focus measurement of the on-axis image spot. These measurements are performed using a visible monochromatic source, i.e. a laser, to avoid unwanted chromatic aberrations. There is a distinct signature pattern that is present in the image spot for MSF error afflicted optics, as can be seen in Figure 1 for the Stage 1 monolith design.

A programmed user-defined surface used with CODE V serves as the basis for our MSF model. This model enables us to simulate the effect MSF error has on the nominal monolithic designs, including calculations of the through-focus spot.

Once the model was verified against empirical measurements, sensitivity analysis and tolerancing was performed on the Stage 3 design for which MSF frequency and amplitude ranges meet an as-built imaging performance metric. The system performance is being specified by Optimax with Strehl ratio.

b) Mid-Spatial Frequency Error Modeling Method

In the monolithic telescope designs, the freeform surfaces are defined using XY polynomials on top of a basic conic surface, with the sag:

$$\begin{aligned} z_{\text{nom}}(x,y) &= z_{\text{conic}}(x,y) + z_{\text{XY}}(x,y) \\ &= \frac{cr^2}{1+\sqrt{1-(1+k)\,c^2r^2}} + \sum_{m=0}^{\infty}\sum_{n=0}^{\infty} c_{m,n}x^m y^n \end{aligned}$$

where c is the surface curvature, $r^2 = x^2 + y^2$, k is the conic constant, and $c_{m,n}$ are coefficients that are determined for each m, n XY pair.

The MSF error on top of these XY polynomial surfaces can be modeled by adding a two-dimensional sinusoidal sag and local slope error across the part:

$$z_{\text{MSF}}(x,y) = A\cos(\omega_x x) + B\cos(\omega_y y)$$

where A and B are ripple amplitudes and ω_x and ω_y are ripple angular frequencies in X and Y, respectively.

Thus, the total sag modeled for XY polynomial freeform surfaces with MSF figure error is the sum of the two equation above:

$$\begin{aligned} z(x,y) &= z_{\text{nom}}(x,y) + z_{\text{MSF}}(x,y) \\ &= \frac{cr^2}{1+\sqrt{1-(1+k)\,c^2r^2}} + \sum_{m=0}^{\infty}\sum_{n=0}^{\infty} c_{m,n}x^m y^n + A\cos(\omega_x x) + B\cos(\omega_y y) \end{aligned}$$

In calculating ray trace data, the surface derivatives with respect to the Cartesian coordinates, x and y, are also needed:

$$\begin{aligned} \frac{\partial}{\partial x} z &= \frac{\partial}{\partial x}\left(z_{\text{conic}} + z_{\text{XY}} + z_{\text{MSF}}\right) \\ \frac{\partial}{\partial y} z &= \frac{\partial}{\partial y}\left(z_{\text{conic}} + z_{\text{XY}} + z_{\text{MSF}}\right) \end{aligned}$$

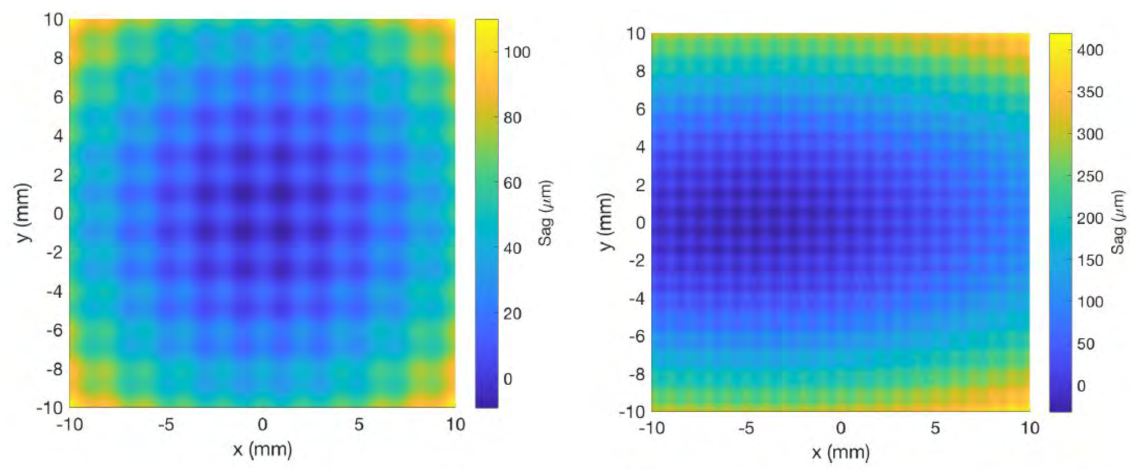

Figure 2: Examples of freeform surfaces containing MSF error created by the MSF model.

This mathematical model is implemented using CODE V via a User-Defined Surface (UDS). The UDS is a dynamic-link library programmed in C++ that when loaded into CODE V will actively return the sag and derivative values for the surface in order for CODE V to perform ray tracing.

Moreover, this mathematical model is designed for *general use* with changeable amplitudes and spatial frequencies in the X and Y dimensions *only* so as to be usable with different optical systems in the future. In other words, the modeled MSF error may not align precisely with a measured surface due to randomness and higher order complication like amplitude and frequencies varying across a dimension. To fine tune our model to fit precisely the MSF surfaces at hand would lose the generalization capabilities of a model usable for other cases. As can be seen in the Results section, the model's surfaces indeed do not precisely match the surface profilometry measurements but do offer a surface that is consistent with the measured dominant amplitudes and frequencies.

c) *Model Verification & Testing*

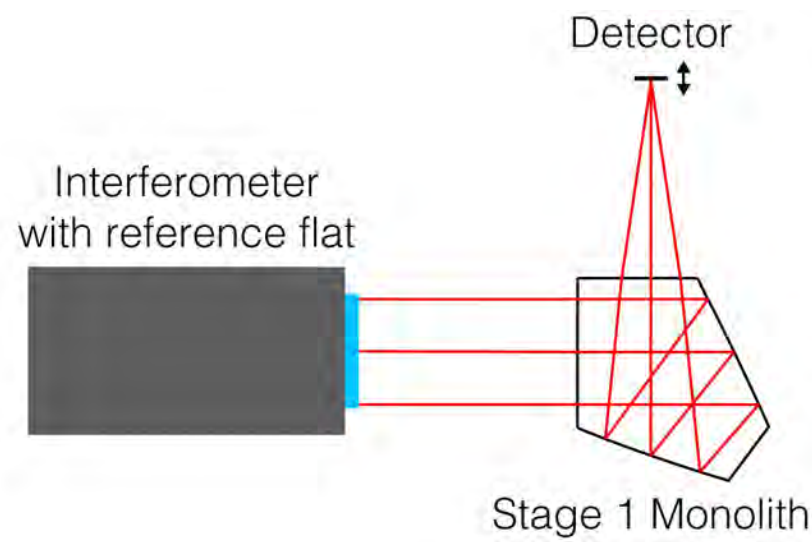

Figure 3: Testing setup for measuring through-focus on-axis spot.

In order to verify the MSF error model, on-axis through-focus measurements of the image spot were taken for the Stage 1 design. A monochromatic laser source was used to avoid chromatic aberration effects. The source used was a Zygo Verifire laser interferometer using a 4-inch plano reference flat. The monolith was placed on a 6 degree of freedom stage and was aligned to the incident planar wavefront using the standard capabilities of the interferometer. Then, the detector - a full frame CMOS sensor - was aligned to the exit face of the monolith and was moved through focus using a linear translation stage. Spot measurements were performed every 1 mm with a smaller increment at best focus. This testing plan is visualized in Figure 3.

d) *Additional analyses*

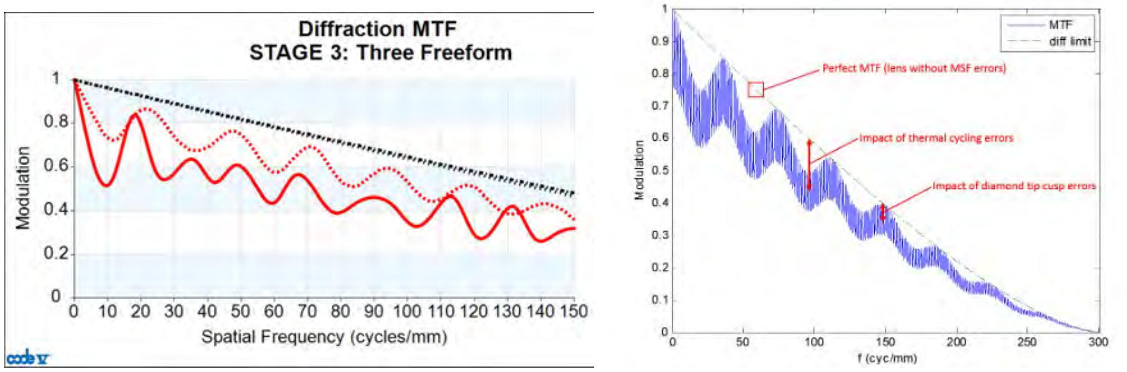

Figure 4: Ripples in the MTF for a system suffering from MSF error. Left: on-axis MTF for Stage 3 monolith design. Right: theoretical example.[6]

As can be seen in the work of Suleski, the presence of MSF error will result in ripples in the MTF curve for the system, as can be seen in Figure 4.[6] This fact was confirmed using the model previously discussed applied to the Stage 3 design. This serves as an additional confirmation of the mathematical model.

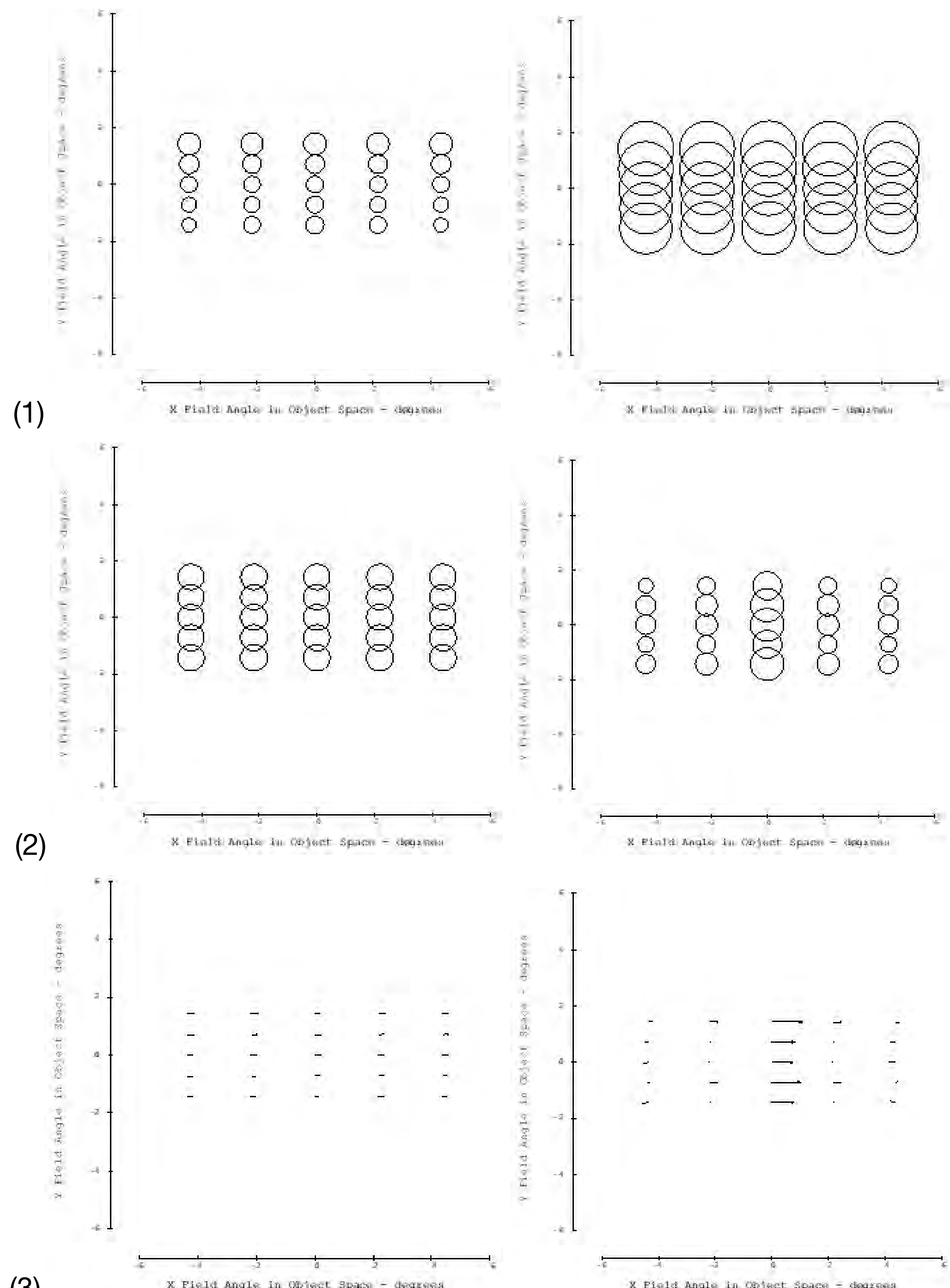

Figure 5: Full field display (FFD) for nominal (left) and MSF afflicted (right) Stage 1 design. (1) RMS wavefront error (waves). (2) Primary spherical aberration(waves). (3) Secondary astigmatism (waves). The FFD clearly depicts what specifically is being affected by the presence of MSF error.

To understand how significant MSF error is on performance, aberration analysis has been conducted on Stage 1 telescope. In order to examine MSF error, the RMS wavefront was measured before and after the MSF error was introduced. In addition, the zernike aberrations' effect on full field from was compared and plotted. Without MSF error, the average RMS size is 0.79 waves. With MSF error, the average RMS size is 2.43 waves, which is a huge drop in performance. To give a perspective, typically diffraction limited system has about 0.07 waves.

Examining aberration individually, there is significant increase in effect of defocus, spherical aberration, coma, secondary astigmatism, and primary tetrafoil after MSF error has put on. On each aberrations, the effect of MSF error scales in some sort of formulaic pattern. Specifically, as shown in Figure 5, in primary spherical aberration and secondary astigmatism MSF error scales sinusoidally on Y field, as well as on X field, but with a different frequency. This is expected, because adding MSF error on to each surfaces is like creating patternized changes to wavefront as it reflects each surfaces, resulting in patternized MSF error effect on each aberration.

As a side note, just because individual aberration contribution is large, it does not mean that that aberration contribution is negatively affecting the system performance. Consequently, because the system is limited by aberrations and MSF error is patternized, it is interesting to think if with right frequency and amplitude, MSF error could have positive effect on aberrations and potentially balance aberrations to minimize the rms spot size.

However, if the system designed supposedly to be diffraction limited, these formulaic pattern of MSF error on each aberrations could only make the system performance worse, because it would most likely to unbalance the aberration contribution. Consequently, it is expected that diffraction limited system performance would be impacted by MSF error more than aberration limited system. We can confirm this by putting similar MSF error on stage 3 telescope and comparing its average rms values before and after. Without MSF error, the average RMS size is 0.066 waves. With MSF error, the average RMS size is 1.45 waves. For stage 3, MSF error increased rms spot size by 21 times. Where as for stage 1, MSF error increased rms spot size by only 3 times, highlighting the expectation.

3. Results

a) Surface profile analysis for Stage 1

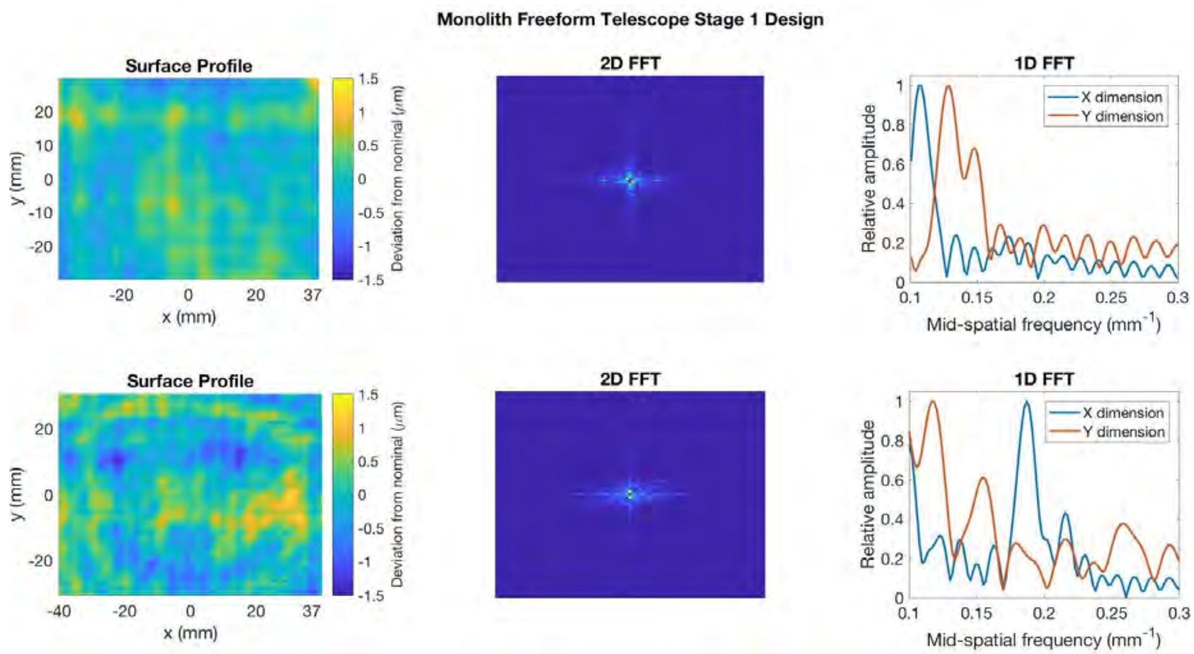

Figure 6: Stage 1 profilometry surface measurements, 2D Fast Fourier Transform (FFT), and 1D FFT. Top: first freeform surface. Bottom row: second surface.

	Spatial frequency, X (mm^{-1})	Spatial frequency, Y (mm^{-1})	PV amplitude, X (µm)	PV amplitude, Y (µm)
Surface 2	0.1062	0.1287	0.3626	0.3321
Surface 3	0.1870	0.1168	0.4774	0.5159

Table 1: Dominant mid-spatial frequencies and peak-to-valley (PV) amplitudes in X and Y for each surface.

High-resolution profilometry measurements for the two freeform surfaces of the Stage 1 design were taken by Optimax. This data is plotted with its 1D and 2D Fast Fourier Transforms (FFT) in Figure 6 with its peak spatial frequencies and amplitudes listed in Table 1. Note that spatial frequencies less than 0.1 mm^{-1} are excluded since these are more on the level of low-spatial frequency error rather than MSF error.

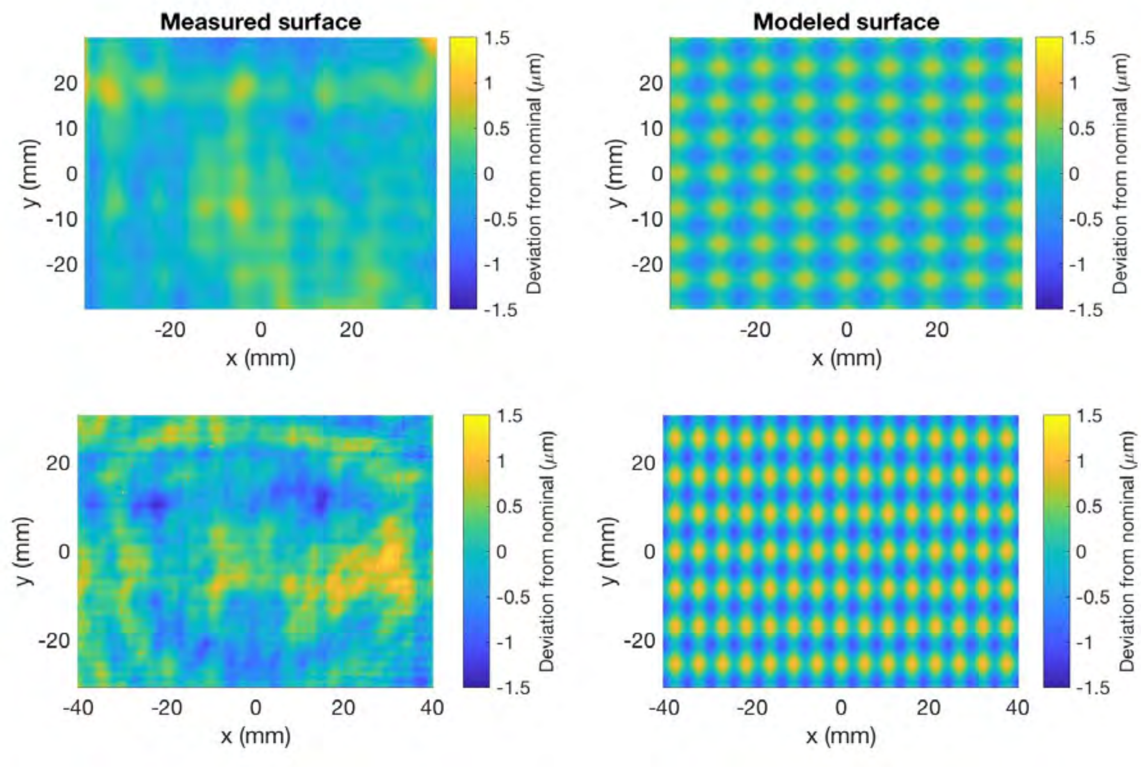

Figure 7: Comparison of measured and modeled surface sag deviation from nominal for the Stage 1 design. Modeled MSF frequencies and amplitudes are those in Table 1. Top: first freeform surface. Bottom: second freeform surface. All plots are on the same color scale.

The mid-spatial frequencies and amplitudes in Table 1 were then applied to the model for the freeform surfaces in Stage 1. The measured and modeled deviation from nominal sag can be seen in Figure 7.

b) Model verification

Now that the characteristic MSF frequencies and amplitudes were applied to the Stage 1 computational model, different aspects of the measured through-focus spots were analyzed.

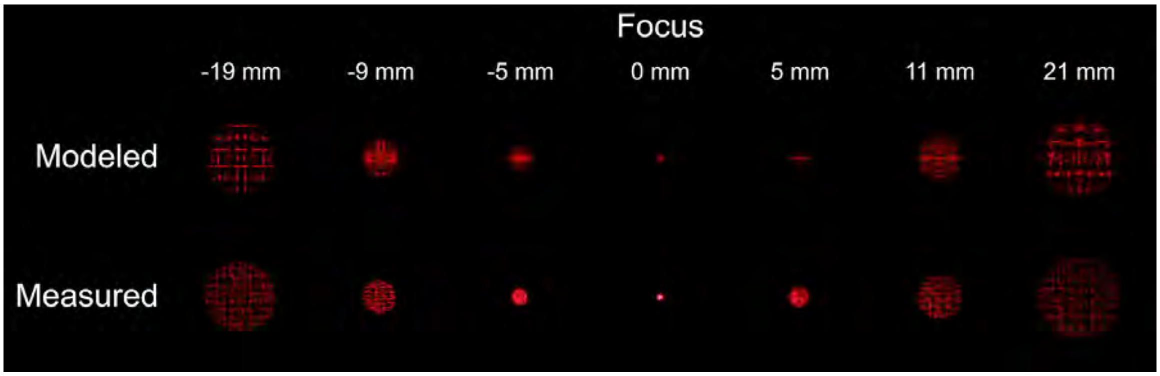

Figure 8: Comparison of modeled and measured image spots through-focus for the Stage 1 design. All spots are on the same relative spatial scale but not the same relative intensity scale. Both modeled and measured spots possess the expected MSF signatures.

First, the spatial characteristics of the modeled and measured spots were compared at different through-focus positions. As can be seen in Figure 8, both the modeled and measured spots contain signatures of MSF error, and both are very similar in shape and size. Both sets of spots contain vertical and horizontal nulls and hot spots. Recall that the MSF model is an approximation using only single frequencies and amplitudes in X and Y, so it was never expected that the sets of spots should match exactly. Some differences are present as the spot decreases in size. This is most likely due to a difference in sampling since the pixel sampling for the measured spots decreases with size while this is not the case for the computational model which has constant sampling regardless of spot size. Overall, the shape and qualitative properties of the two sets of spots is considered very strongly correlated and serves as strong support for the proposed MSF model.

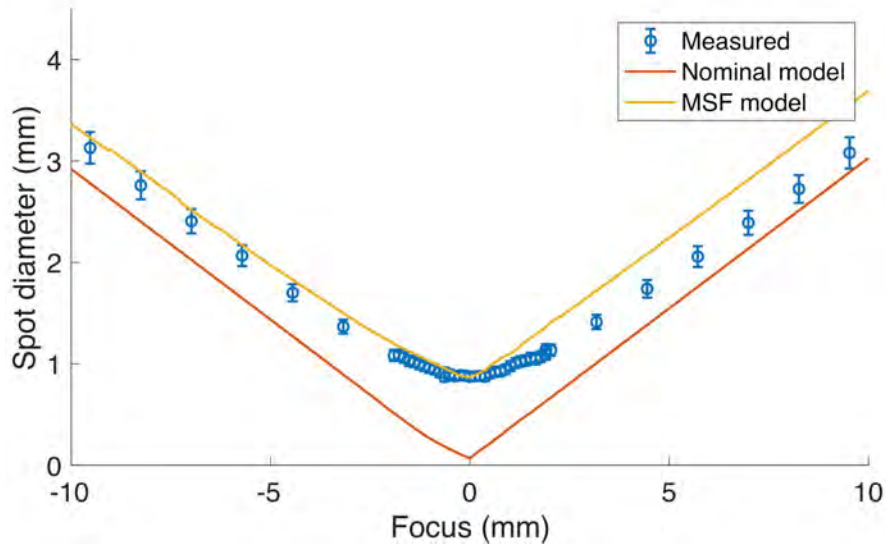

Figure 9: Spot diameter for Stage 1 design. Measured spot diameters correlate closely to those predicted by MSF model.

Next, more quantitatively, the diameter of the produced image spots were evaluated. By knowing the pixel pitch of the CMOS detector used for the empirical measurements (6.55 micron), a physical spot diameter can be determined through the measured pixel size of the spots. Meanwhile, the modeled spot diameters waweres calculated using CODE V, first the nominal Stage 1 design and again with the MSF ripples included. The comparison of the measured and modeled spot diameters can be seen in Figure 9. The measured spots correlate strongly with what the MSF model predicts, especially at best focus. Moreover, the measured spot diameters are symmetrical through focus, as one would expect for a spherical converging and then diverging wavefront. Meanwhile, the model for both nominal and MSF designs predicts the rate at which the spot diameter increases to be slightly greater on the far side of focus, resulting in slight asymmetry of the model curves. This is the cause of the deviation of measured and modeled diameters for positive focus values. The reason for this is not entirely known but is thought to be due to diffraction effects overlooked by CODE V. Overall, the measured spot diameter closely matches what the MSF model predicts for most of the focus range and especially around best focus, a strong confirmation of the computational model.

Overall, the conclusion of the empirical through-focus spot measurements is that the results strongly confirm the validity of the proposed computational MSF model. Now that the model has been proven to be representative of MSF errors, sensitivity analysis and tolerancing can now be performed.

b) Sensitivity analysis & tolerancing

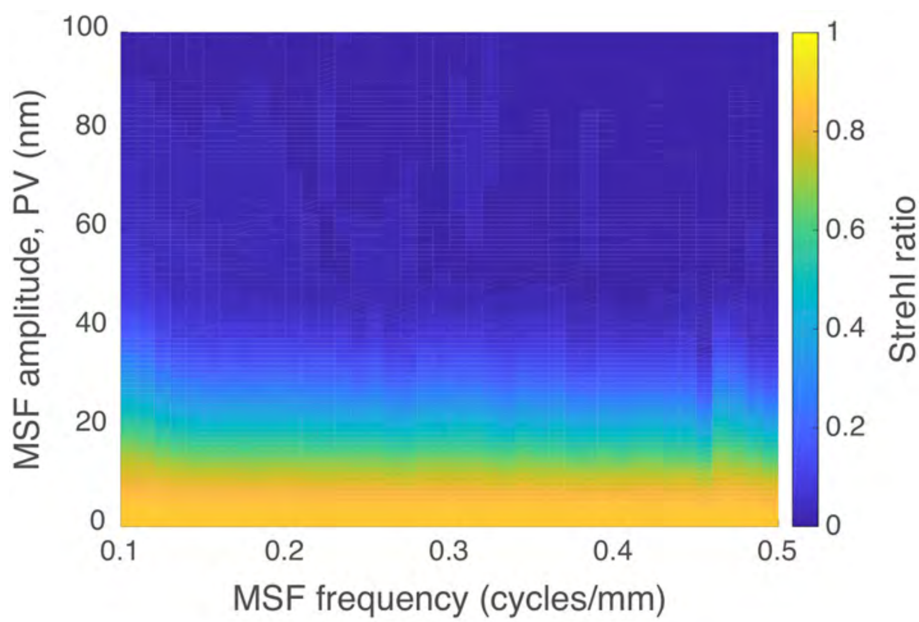

Figure 10: Strehl ratio as a function of different MSF frequencies and amplitudes for the Stage 3 diffraction-limited design. Analysis performed for the on-axis field point.

Now that the validity of the MSF model has been proven, the model can be used to achieve the overarching objective of the project: determining how MSF error affects imaging performance and, specifically, how much is tolerable to achieve a certain performance specification. This analysis was performed on the Stage 3 design for two reasons: (1) it is the best performing of the three monolithic telescopes, and (2) its fabrication is not yet complete.

As provided by Optimax, the performance metric employed was Strehl ratio which is the ratio of the aberrated point spread function (PSF) to the unaberrated, diffraction-limited PSF. On-axis, the Strehl ratio of the nominal Stage 3 design was 0.86 and typically a Strehl ratio of greater than 0.8 is considered diffraction limited. Using the MSF model, combinations of different MSF frequencies and amplitudes were applied to the Stage 3 MSF model, and the Strehl ratio was calculated. These frequencies and amplitudes were applied evenly in the X and Y dimensions as well as on all three of the Stage 3 freeform surfaces. The results can be seen in Figure 10. Interestingly, MSF ripple amplitude has a considerable effect on performance while MSF frequency has almost no effect. Also, in order to maintain diffraction-limited performance, the MSF amplitude, PV, must be approximately 10 nm or less on all freeform surfaces. This is considerably smaller than the MSF ripples measured on the Stage 1 monolith which have PV amplitudes of 1-2 microns.

4. Project Details

a) Designs

There are three different stages of monolithic freeform telescope designs.

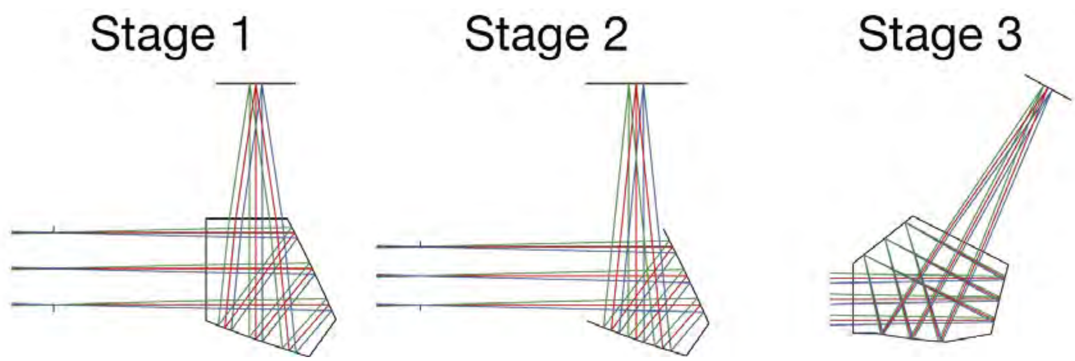

Figure 11: Three monolithic freeform telescope designs.

Stage 1 is prismatic, contains two plano windows and two freeform surfaces, and is not diffraction limited.

Stage 2 is C-shaped, contains the same two freeform surfaces as Stage 1, and is not diffraction limited.

Stage 3 is prismatic and contains two plano windows, three freeform surfaces, and is diffraction limited.

The fabrication of:

> Stage 1 and Stage 2 is completed.
>
> Stage 3 is in process. Grinding is complete, and polishing and coating will be completed early in summer of 2018.

Design Specifications:

	Stage 1	**Stage 2**	**Stage 3**
Half field of view, Y (°)	4.365	4.365	4.365
Half field of view, X (°)	1.431	1.431	1.431
Entrance pupil diameter (mm)	50	50	50
Design wavelength (nm)	633	633	633
Effective focal length (mm)	168.338	248.732	227.082
Material	Silica	Silica	Silica
Number of freeform surfaces	2	2	3
Design style	Prism	C shape	Prism
Diffraction limited performance?	No	No	Yes
Fabrication complete?	Yes	Yes	No

Table 2: System specifications for three monolithic freeform telescope designs. The fabrication of Stage 3 is in process and is expected to be complete early in the summer of 2018.

b) Fabrication Methods for Monolith Designs

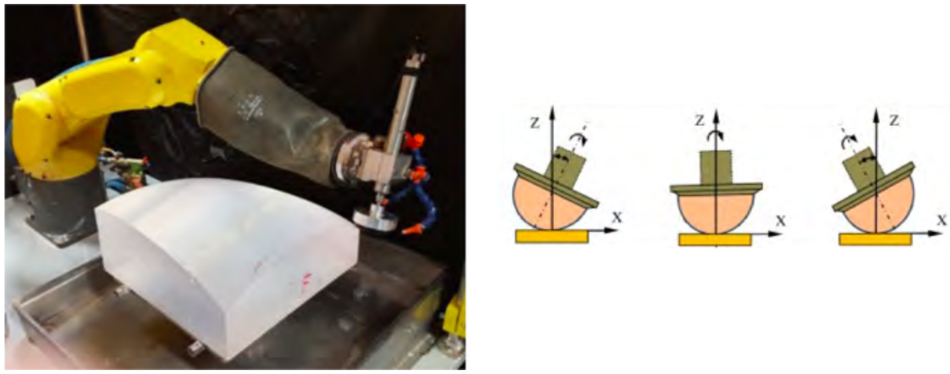

Figure 12: Grinding and polishing methods for monolithic telescope designs. Left: contour grinding. Right: bonnet polishing.[4]

The surfaces of the monolithic freeform telescopes are being ground with a robotic arm using a contour bound-abrasive diamond tool, as in Figure 12. The surfaces are being polished using a sub-aperture bonnet technique typical of Zeeko polishers. Both of these methods are sub-aperture optical fabrication methods and, therefore, leave residual MSF error. Qualitative evidence of this MSF error can be seen in Figure 1 where in-homogeneity is evident in the out of focus image spot for the Stage 1 design. This could be attributed to the MSF errors on both of the freeform surfaces.

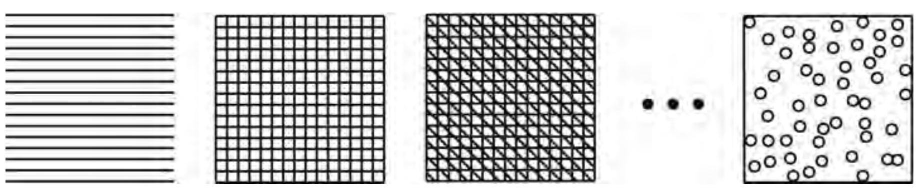

Figure 13: Different number of overlaps of linear MSF patterns, ultimately yielding a randomized surface pattern.

In the world of optical fabrication, MSF error is a looming grey area where not much is well defined about its effect on performance, yet a variety of techniques exist to mitigate the presence of MSF. The technique being used by Optimax to mitigate the MSF features on the monolithic freeform surfaces consists of repeatedly raster polishing the same surface but with the raster path oriented at different angles, as in Figure 13. The result of repeatedly overlapped linear patterns is a pattern of pseudo-random clusters of 2D Gaussian "islands." This effect can be seen in the surface measurements in Figure 6. These islands can be approximately modelled sing a 2D grid of linear sinusoidal gratings being applied to a surface.

c) Mid-Spatial Frequency Error (MSF) Characteristics

A variety of different MSF parameters can affect imaging performance, as listed in Table 3 and depicted in Figure 14.

Parameter	*Description*
Frequency	The number of ripple cycles per unit length on a surface
Amplitude	The ripple height and depth
Style	Linear, concentric ripples, or 2D Gaussian “islands”
Relative orientation	Angular orientation of ripples on surface
Surface number	The location of surface within a system

Table 3: Five parameters defining effect mid-spatial frequency figure error has on the point spread function.

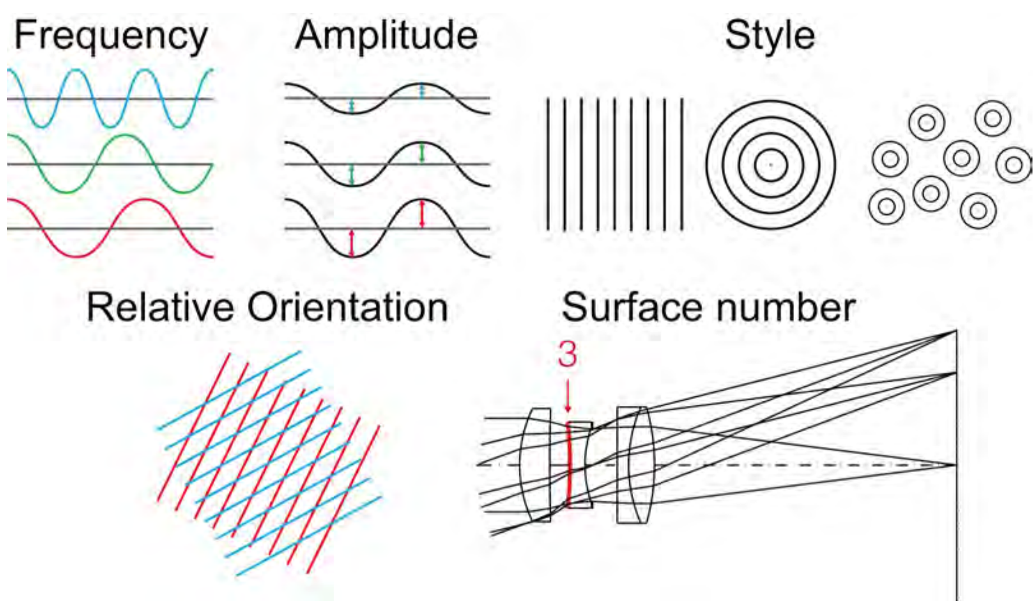

Figure 14: Depiction of five parameters defining the effect mid-spatial frequency figure error has on imaging performance.

f) Other Considerations

Depending on the nominal performance of the monolithic telescope design in question, MSF may have a bigger effect on one design compared to another. For Stage 1, for example, which is far from diffraction limited, the effect of MSF error may be minimal relative to overall performance while prominent MSF may affect the diffraction limited Stage 3 performance greatly.

Furthermore, it should be noted that comparing simulated results from our MSF model with empirically measured results may not yield a direct correlation. Since the realm of our analysis is limited to MSF figure error and ignores other design sensitivities including figure, irregularity, thickness, material, surface tilt, etc., other errors from fabrication will also affect imaging performance. After exhausting all options to reconcile our model with measurements, our backup plan will be to rely on the model since it has received some form of verification through the work of John Tamkin.[1-3]

5. Hajim Design Day

Figure 15: Hajim Design Day 2018. Photo credit to University of Rochester.

For the Hajim Design Day on May 4th, 2018, we displayed the completed Stage 1 prototype alongside our poster presentation and computational model.

6. Acknowledgements

Thank you to our faculty advisor Professor Jannick Rolland who has been very helpful as well as Professor Wayne Knox.

7. References

1. Tamkin, John M., and Tom D. Milster. "Effects of Structured Mid-Spatial Frequency Surface Errors on Image Performance." *Applied Optics*, vol. 49, no. 33, 2010, pp. 6522.

2. Tamkin, John M., William J. Dallas, and Tom D. Milster. "Theory of Point-Spread Function Artifacts due to Structured Mid-Spatial Frequency Surface Errors." *Applied Optics*, vol. 49, no. 25, 2010, pp. 4814.

3. Tamkin, John M., Tom D. Milster, and William Dallas. "Theory of Modulation Transfer Function Artifacts due to Mid-Spatial-Frequency Errors and its Application to Optical Tolerancing." *Applied Optics*, vol. 49, no. 25, 2010, pp. 4825.

4. Rogers, John R. Slope Error Tolerances for Optical Surfaces, vol. 10316, SPIE, 2007, doi:10.1117/12.725057.

5. H. Aryan, C. J. Evans, and T. J. Suleski, "On the Use of ISO 10110-8 for Specification of Optical Surfaces with Mid-Spatial Frequency Errors," in *Optical Design and Fabrication 2017 (Freeform, IODC, OFT)*, OSA Technical Digest (online) (Optical Society of America, 2017), paper OW4B.2.

6. Jason A. Shultz, Hamidreza Aryan, Joseph D. Owen, Matthew A. Davies, and Thomas J. Suleski. “Impacts of sub-aperture manufacturing techniques on the performance of freeform optics.”